Published in final edited form as:
J Neuroimmune Pharmacol. 2012 December ; 7(4): 991–1001. doi:10.1007/s11481-012-9403-y.

CEREBROVASCULAR TOXICITY OF PCB153 IS ENHANCED BY BINDING TO SILICA NANOPARTICLES

Bei Zhang[1,2,*], **Lei Chen**[2,†], **Jeong June Choi**[2,*], **Bernhard Hennig**[1,3], and **Michal Toborek**[1,2,*]

[1]Graduate Center for Nutritional Sciences, University of Kentucky, Lexington, KY

[2]Department of Neurosurgery, University of Kentucky, Lexington, KY

[3]College of Agriculture, University of Kentucky, Lexington, KY

Abstract

Environmental polychlorinated biphenyls (PCBs) are frequently bound onto nanoparticles (NPs). However, the toxicity and health effects of PCBs assembled onto nanoparticles are unknown. The aim of this study was to study the hypothesis that binding PCBs to silica NPs potentiates PCB-induced cerebrovascular toxicity and brain damage in an experimental stroke model. Mice (C57BL/6, males, 12-week-old) were exposed to PCB153 bound to NPs (PCB153-NPs), PCB153, or vehicle. PCB153 was administered in the amount of 5 ng/g body weight. A group of treated animals was subjected to a 40 min ischemia, followed by a 24 h reperfusion. The blood-brain barrier (BBB) permeability, brain infarct volume, expression of tight junction (TJ) proteins, and inflammatory mediators were assessed. As compared to controls, a 24 h exposure to PCB153-NPs injected into cerebral vasculature resulted in significant elevation of the BBB permeability, disruption of TJ protein expression, increased proinflammatory responses, and enhanced monocyte transmigration in mouse brain capillaries. Importantly, exposure to PCB153-NPs increased stroke volume and potentiated brain damage in mice subjected to ischemia/reperfusion. A long-term (30 days) oral exposure to PCB153-NPs resulted in a higher PCB153 content in the abdominal adipose tissue and amplified adhesion of leukocytes to the brain endothelium as compared to treatment with PCB153 alone. This study provides the first evidence that binding to NPs increases cerebrovascular toxicity of environmental toxicants, such as PCB153.

Keywords

blood-brain barrier; polychlorinated biphenyls; silica nanoparticles; stroke; tight junctions

INTRODUCTION

Polychlorinated biphenyls (PCBs) are organochlorinated chemicals that were mass produced for industrial usage in the U.S. for approximately 50 years (Yamada et al., 1997). Environmental exposure to PCBs is ongoing as a result of continued use and disposal of products containing these toxicants (Prince et al., 2006), as well as prevalent bioaccumulation of PCBs in the biosphere and in the food chain (Norstrom et al., 2010). PCBs present in the environment can bind to organic particles in water, sediments, soil, and

Corresponding Author: Michal Toborek, MD, PhD; Department of Biochemistry and Molecular Biology, University of Miami School of Medicine, Gautier Bldg., Room 517, 1011 NW 15th Street. Miami, FL 33136. Phone# 305-243-0230, mtoborek@med.miami.edu.
*Current Address: Department of Biochemistry and Molecular Biology, University of Miami School of Medicine, Miami, FL
†Current Address: Department of Neuroscience, Mount Sinai School of Medicine, New York, NY

Conflict of interest: The authors declare that they have no conflict of interest.

atmospheric particulates. In contaminated areas in New Bedford Harbor (MA), average PCB concentration was determined to be 2.3 mg/l in water and 351 μg/kg in sediments (Lake et al., 1995). The average PCB levels in the air and soil samples collected in Anniston (AL) were 62.8 ng/m^3 and 2.8 mg/kg, respectively (ATSDR, 2000). Importantly, elevated environmental levels of PCBs were associated with increased levels in serum in the exposed population and higher prevalence to disease development (Goncharov et al., 2010; Silverstone et al., 2012). Evidence suggests that exposure to PCBs may increase the incidence of stroke (Shcherbatykh et al., 2005) and worsen stroke outcome (Dziennis et al., 2008). Importantly, highly chlorinated ortho-PCBs preferentially accumulate in the brain and thus induce prominent neurotoxic effects (Saghir et al., 2000). The most representative compound from this group is 2,2′,4,4′,5,5′-hexachlorobiphenyl (PCB153), which is common in environmental samples and accounts for 15–30% of total PCB content in most human samples (Hansen, 1998; Saghir et al., 2000).

When released from environmental sources, PCBs can be adsorbed onto suspended particles present in the air, such as ultrafine (nano-size particles) or fine particles. It has been reported that PCBs can bind to indoor and outdoor dust with the particle size ranging from 0.95 μm to 1.5 μm (Roberts and Dickey, 1995; Chrysikou et al., 2009; Fu et al., 2009). Nanoparticles (NPs) and fine particles are able to penetrate the alveolar-capillary barrier of the lung to access circulating blood cells (e.g. erythrocytes) (Valavanidis et al., 2008). Results from animal experiments indicated that ultrafine particles can translocate into the systemic circulation (Nemmar and Inuwa, 2008) and the brain (Oberdorster et al., 2004) through inhalation or nasal instillation. Thus, particulate components from the ambient air may act as effective carriers for various environmental pollutants entering the brain.

The blood-brain barrier (BBB) is a chemical and physical barrier composed of brain endothelial cells, which are connected by tight junctions (TJs), and interact with other cells and basement membrane of the neurovascular units (Alexander and Elrod, 2002; Abbott et al., 2006). The presence of intact TJs is essential in maintaining a functional BBB (Alexander and Elrod, 2002). Disruption of the BBB is associated with several acute and chronic disorders of the central nervous system (CNS), including stroke, ischemia/reperfusion, hypoxia/reoxygenation and cerebrovascular dysfunction (Fullerton et al., 2001; Hawkins and Davis, 2005; Abbott et al., 2006). In addition, age and conditions linked to aging, including hypertension and brain ischemia, can contribute to alterations of BBB functions. The BBB contains the specialized carriers for glucose, amino acids, purine bases, nucleosides and other substances, which ensure adequate delivery of nutrients, hormones, and neurotransmitters. At the same time, the brain endothelium acts as an effective barrier to prevent the circulating toxic agents entering the brain parenchyma. Thus, age-related BBB dysfunction may impair the transport of nutrients and metabolites to the brain, whereas the leaky barrier allows the circulating toxicants access the brain tissue. Moreover, genetic variances may affect the BBB functions and contribute to the disease etiology. For instance, heterozygous mutation in the glut1 gene results in glucose transporter (GLUT-1) deficiency syndrome (Hawkins and Egleton, 2008), which impairs the transport of glucose across the BBB. The cells composing the BBB can also interact with NPs. It was demonstrated that NPs have ability to cross the BBB and accumulate in brain parenchyma (Calderon-Garciduenas et al., 2008).

With the robust development of nanotechnology, nanotoxicity is also gaining increased attention. Surface modifications of NPs markedly affect their biological and toxicological properties. For example, neutral and anionic NPs at low concentrations appear to have no effect on BBB integrity, whereas high concentrations of positively or negatively-charged NPs disrupted the BBB. Anionic NPs were preferentially taken up by the brains as compared to neutral or positively-charged NPs (Lockman et al., 2004). Other unique functionalities of

NPs, including high surface area, make NPs a target for other environmental contaminants, such as PCBs. Nevertheless, there are no research reports on cerebrovascular toxicity of PCBs bound to NPs. In the present study, we demonstrate for the first time that such binding results in increased cerebrovascular toxicity of PCB153, leading to enhanced brain injury in experimental stroke model.

MATERIALS AND METHODS

Characterization of silica NPs and binding PCB153 to NPs

Silica NPs were purchased from NanoAmor (Houston, TX). In order to determine the effect of different media on particle size distribution, particles were dispersed in distilled water, phosphate buffered saline (PBS), or EBM-2. Then, the diameter size and the polydispersity index (PDI) were assessed by dynamic light scattering (DLS) using a Malvern Instruments Zetasizer Nano ZS.

In order to assemble PCB153 onto NPs, silica NPs (80 mg) were mixed with 10 mg of PCB153 (2,2′,4,4′,5,5′-hexachlorobiphenyl, AccuStandard, New Haven, CT) in acetone and sonicated. Acetone was allowed to evaporate and the mixture of NPs with PCB153 was resuspended in water PBS or EBM-2. Sonication was applied during the process to minimize the particles' aggregation. The suspension was centrifuged at 12,000 rpm for 5 min. The supernatant was collected to analyze the final concentration of PCB153 by gas chromatography/mass spectrometry (GC/MS). Control NPs were prepared using the same procedure, without adding PCB153.

Animals and experiment groups

All experiments were performed following the protocol approved by the National Institutes of Health Guide for the Care and Use of Laboratory Animals. Mice (C57BL/6, 12-week-old, male) were anesthetized with isoflurane and then infused with: a) PCB153 bound to silica NPs (PCB153-NPs), b) PCB153 dissolved in 0.01% DMSO (PCB153), c) silica NPs alone, or d) vehicle (DMSO or PBS). Sham controls were subjected to surgical procedures without additional treatment. All injections were performed through the internal carotid artery (ICA) to ensure drug delivery into the brain. PCB153 was administered in the amount of 5 ng/g body weight. This design simplified the routes of exposure and potential surface modification of NPs, which may occur when passing the gastrointestinal track, skin, or airway passages. Direct injections into the bloodstream allowed for precise dosing to evaluate whether binding of PCB153 to NPs influences their toxicological properties.

In selected experiments, mice were exposed to PCB153-NPs or PCB153 alone by oral gavage at the dose of 5 ng/g once a day for 30 days. Such treatment mimics chronic exposure to PCBs through food chain. Adipose tissue was then collected and analyzed for PCB153 levels.

Surgical procedures

Injections via the internal carotid artery (ICA) and the installation of the vessel port were performed as described earlier by our group (Chen et al., 2009). The focal ischemia stroke model was based on a 40 min occlusion of the middle cerebral artery (MCA), confirmed by a sharp decline in cerebral blood flow, followed by 24 h reperfusion. Then, the brains were removed, sectioned into 1 mm slides, and the infarct area was visualized by 2,3,5-triphenyltetrazolium chloride (TTC) staining. The infarct volume was quantified by ImageJ analysis software as described earlier (Zhang et al., 2010).

Cranial windows were installed to observe leukocyte interactions with cerebral vessels. Under anesthesia, the left parietal bone was exposed by a midline skin incision, followed by a craniotomy (2.5 mm diameter) 2.5 mm posterior from the bregma and 2.5 mm lateral from the midline. The dura mater was removed to expose the underlying pial vasculature. A glass coverslip was placed and sealed with dental cement over the exposed brain tissue, which was suffused with artificial cerebrospinal fluid. Attachment of leukocyte to the brain endothelium was assessed as described earlier (Chen et al., 2011) using rhodamine 6G (Rho6G) chloride to label circulating leukocytes.

Monocyte transmigration assay *in vivo*

Murine monocyte/macrophage cells J774.1 were cultured in DMEM medium (Invitrogen, Carlsbad, CA) supplemented with 10% FBS and antibiotics (penicillin, 100 U/ml; and streptomycin, 100 μg/ml, Invitrogen). Monocytes were labeled with 20 μM CFDA-SE (Vybrant CFDA-SE Cell Tracer Kit, Invitrogen), a dye which passively diffuses into cells and yields fluorescence when its acetate groups are cleaved by intracellular esterases. Mice were injected into the ICA with labeled monocytes at a concentration of 0.5×10^6 cells, which were then allowed to circulate for 24 h. Brains were sliced (20 μm thick) and stained to visualize the interaction of labeled monocytes with the brain endothelium. Staining for claudin-5 was employed to visualize the brain capillaries. Images were acquired using a Nikon fluorescence microscope (Nikon, Melville, NY) equipped with a SPOT RT camera and software (Diagnostic Instruments, Sterling Heights, MI).

Analysis of PCB153 levels in adipose tissue

Tissue levels of PCB153 were analyzed as described previously (Sipka et al., 2008). Briefly, adipose tissue samples (0.2–0.5 g) were spiked with surrogate standards (PCB65 and PCB166) and mixed with 1.0 g diatomaceous earth. The mixtures were then homogenized and extracted with ASE 200 accelerated solvent extractor (Dionex Corporation, Sunnyvale, CA). After extraction with hexane, the extracts were concentrated using Rotavapor, vortexed thoroughly, left overnight to achieve phase separation, and the hexane layer containing PCB153 was collected. The extracted aliquots were further concentrated and 10 μl of 1.0 ng/μl of internal standard PCB209 was added to each sample and transferred to a glass microvial for analysis. Gas chromatographic analysis was performed with a GC-μECD system (Agilent GC 6890N, autosampler G2913A, μECD detector) (Agilent Technologies, Santa Clara, CA). PCB153 was identified on the basis of the retention time relative to standards. Quantification was achieved based on calibration curves obtained using PCB standards, the recovery efficiency calculated from the surrogates, and the sample weight.

BBB permeability assay

Animals were injected i.p. with 200 μl 10% sodium fluorescein in PBS. Fifteen minutes later, blood was collected via cardiac puncture. Animals were transcardially perfused with 0.9% saline, the brains were harvested, and homogenized in PBS (1/10; w/v). Fluorescence was determined using excitation at 485 nm and emission at 530 nm. The permeability results were presented as a ratio of brain to plasma fluorescence intensity.

Immunoblotting and immunoreactivity

Brain microvessels were isolated as described previously (Seelbach et al., 2010) and either lysed for immunoblotting or smeared on the glass slides for immunoreactivity assessments. Lysed microvessels (50 μg protein per sample) were electrophoresed on 4–15% Tris-HCl Ready SDS-polyacrylamide gel (Bio-Rad Laboratories, Hercules, CA), transferred onto PVDF membranes (Bio-Rad Laboratories), and incubated with specific primary antibodies. Anti-occludin and anti-claudin-5 antibodies were purchased from Invitrogen, anti-actin

antibody was from Sigma, and all secondary antibodies were from Santa Cruz Biotechnology.

Brain microvessels smeared on the glass slides were incubated with anti-occludin and anti-claudin-5 antibodies for tight junction (TJ) immunoreactivity studies.

Real-time RT-PCR

Freshly isolated microvessels were resuspended in 200 μl of TRIZOL reagent (Invitrogen) and total RNA was extracted according to the manufacturer's instructions. Then, 1 μg of RNA was reverse-transcribed using the Reverse Transcription System (Promega, Madison, WI). PCR amplification was performed using 3 μl of RT product, Taqman Universal PCR Master Mix (Applied Biosystems, Foster City, CA), and the pre-developed primer pairs and Taqman probes (Applied Biosystems) in a total volume of 25 μL. Expression of mRNA was calculated and analyzed by the comparative C_T method as described earlier (Lee et al., 2004).

Cultures of human brain microvascular endothelial cells and *in vitro* transendothelial migration

Human brain microvascular endothelial cells (hCMEC/D3 cell line) were cultured as described previously (Zhong et al., 2008). For transendothelial migration, 1×10^5 hCMEC/D3 cells were cultured on a Transwell filter until reaching confluency. Treatment factors were the same as in animal experiments; however, final concentration of PCB153 was 1.6 μM. Human monocytic THP-1 cells were stained with calcein acetoxymethyl (calcein AM) (5 μM) for 15 min and added in the amount of 2.5×10^5 on top of hCMEC/D3 monolayers for 4 h at 37 °C. Fluorescence originating from the migrating THP-1 cells was measured in 200 μl aliquots collected in the lower compartment of the Transwell system at 485 nm excitation and 530 nm emission.

Statistical analysis

Statistical analysis was completed by using Sigma-Stat 2.03 (SPSS, Chicago, IL). One-way ANOVA, followed by Student-Newman-Keuls *post hoc* test or two-tailed Student's t-test, was used to compare mean responses among the treatments. A statistical probability of $p < 0.05$ was considered significant.

RESULTS

Characterization of NPs and PCB153-NPs

Nanoparticles are known to agglomerate in aqueous solutions. Both NPs and PCB153-NPs agglomerated in water PBS and EBM-2 generating aggregates with the average hydrodynamic diameter of ~250 nm for PCB153-NPs and ~350 nm for silica NPs alone (Table 1). Data reported here are based on Cumulants analysis. Z-average diameter is the mean diameter based on the intensity of scattered light, and the PDI describes the width of the particle size distribution, calculated as $PDI=\sigma^2/Z_D^2$, where σ is the standard deviation and Z_D is the Z average mean size. An increase in the Z-average diameter is an indication of particle aggregation.

As shown in Table 1, the size and PDI of NPs and PCB153-NPs vary in different media. Particles dispersed in PBS and EBM-2 displayed higher PDI value than in water, indicating less uniform dispersion. This may attribute to the ionic strength (IS), pH, or interaction of particles with serum proteins in cell culture medium. Therefore, during material preparation NPs were first dispersed in water and then diluted to final concentration in PBS.

Disruption of TJ protein expression and the BBB integrity is enhanced in mice exposed to PCB153-NPs

TJs are critical elements that regulate the integrity of the BBB. There was a tendency towards diminished levels of occludin after exposure to NPs or PCB153 alone; however, quantified results indicated that these changes did not reach statistical significance. Importantly, administration of PCB153-NPs resulted in a significant decrease in expression of occludin and claudin-5 in brain microvessels (Figures 1A and 1B, respectively) as determined by immunoblotting and immunoreactivity.

Alterations of TJ molecular properties have been associated with disruption of BBB integrity (Abbott et al., 2006). Therefore, we evaluated the influence of PCB153 and/or NPs on the BBB function using an assay based on permeability of a fluorescent marker sodium fluorescein. As indicated in Figure 2, exposure to PCB153-NPs significantly increased the BBB permeability. Such effects were not observed in animals treated with equimolar amount of PCB153 or NPs alone.

Exposure to PCB153-NPs potentiates inflammatory responses in brain capillaries

Stimulation of proinflammatory responses is both the prominent feature of PCB-induced toxicity in the brain (Sipka et al., 2008) and an important element of stroke pathology. Therefore, we determined the effects of PCB153 and/or NPs on mRNA expression of proinflammatory cytokines tumor necrosis factor-α (TNF-α) and interleukin-1β (IL-1β) as well as adhesion molecules intercellular adhesion molecule-1 (ICAM-1) and vascular cell adhesion molecule-1 (VCAM-1) (Figure 3). Exposure to NPs alone did not affect expression of these inflammatory mediators. Treatment with PCB153 alone significantly increased mRNA levels of TNF-α, IL-1β, and ICAM-1 but not VCAM-1. Importantly, exposure to PCB153-NPs resulted in significant elevation of mRNA of all proinflammatory mediators assessed in the present study as compared to both controls and PCB153 alone treated mice.

Exposure to PCB153-NPs induces transcapillary migration of monocytes

Because disruption of the barrier function of the brain endothelium is associated with migration of inflammatory cells into the brain, we evaluated these effects in mice exposed to PCB153 and/or NPs. Mice were injected through the ICA with mouse-derived monocytic J744.1 cells labeled with CFDA-SE. Brain slices were also stained for claudin-5 to visualize brain microvessels. Figure 4A indicates enhanced numbers of monocytic clusters in brain microvessels of mice treated with PCB153-NPs as compared to animals exposed to PCB153 alone. No attachment of labeled monocytes was detected in NP- or vehicle-treated animals.

To further confirm these effects, in vitro studies were performed using human brain endothelial cells co-cultured with human monocytic THP-1 cells. As shown in Figure 4B, treatment with PCB153-NPs, but not with PCB153 or NPs, enhanced transmigration of THP-1 cells.

Exposure to PCB153-NPs potentiates brain injury in the experimental stroke model

We next investigated how binding to NPs can affect toxicity of PCB153 in an experimental stroke model based on middle cerebral artery occlusion (MCAO). Mice were injected with vehicle, PCB153 and/or NPs, into cerebral circulation. Twenty four hours later, the animals were subjected to a 40 min MCAO, followed by a 24 h reperfusion. The infarct volume was evaluated using TTC staining. As indicated in Figure 5, exposure to PCB153-NPs significantly increased the infarct volume induced by ischemia/reperfusion as compared to all other treatment groups.

Long-term exposure to PCB153-NPs stimulates accumulation of PCB153 in adipose tissue and potentiates leukocyte attachment to the cerebral vessels

In the final series of experiments, we changed the route of exposure and evaluated the effects of chronic (30 days) oral exposure to PCB153 and/or PCB153-NPs. Treatment with PCB153-NPs resulted in a significantly higher PCB153 accumulation in adipose tissue collected from abdominal cavity as compared to exposure to PCB153 alone (Figure 6A). Importantly, a chronic exposure to PCB153-NPs resulted in enhanced aggregation of leukocytes in brain vessels and perivascular space as visualized through cranial window (Figure 6B). In contrast, chronic treatment with subtoxic levels PCB153 alone did not affect leukocyte aggregation in cerebral vessels.

DISCUSSION

The transport modes of PCBs in the environment are multifarious, including binding of environmental PCBs to particulate matter (PM) (Nisbet and Sarofim, 1972). In the current study, we hypothesized that such a binding may change toxicological properties of PCBs and influence risk assessment. To address this hypothesis, we evaluated cerebrovascular toxicity of PCB153 bound to silica NPs. The choice of PCB153 was based on the fact that it is one of the most prominent PCB congeners in the environment. Moreover, *ortho*-substituted PCBs, such as PCB153, accumulate in the CNS (Saghir et al., 2000; Sipka et al., 2008). PM collected and analyzed in environmental samples is physically and chemically complex, making analyses of the biological effects of air pollution challenging. In contrast, engineered NPs are mono-dispersed and chemically pure. We used silica NPs as PCB153 carrier due to abundance of silica in the environment. Synthetic silica NPs, being chemically inert, are generally regarded as safe (Campelo et al., 2009) and have been approved for use as food or animal-feed ingredient as well as in diagnostic and biomedical research (Napierska et al., 2009). Importantly, silica NPs employed in the present study were in the similar size range as particles present in the environment.

Once deposited, the fate of NPs depends on their chemical structure and targeted organs. NPs can reach the CNS through the sensory nerves embedded in the airway epithelia (Oberdorster et al., 2004), and/or directly through the BBB (Borm et al., 2006; Peters et al., 2006). While specific NPs can be biodegraded and/or cleared from tissues via the gastrointestinal tract, lymphatic system, and blood circulation, we demonstrated that NPs, such as nano-alumina can still be detected in the brain several days after the initial exposure, causing long lasting effects (Chen et al., 2012).

Results of the present study indicate that animals exposed to PCB153 bound to silica NPs exhibit a dramatic increase in BBB permeability and decrease of TJ protein expression, effects that are not observed in animals exposed to an equal amount of PCB153 alone. Although specific mechanisms of PCB153-NP-induced disruption of BBB integrity are not known, redox-responsive reactions might be involved in this event. The brain is an organ that is highly vulnerable to oxidative stress due to its high content of iron and lipids, high oxygen consumption, and relatively low capacity of antioxidant defenses (Seelbach et al., 2010). Such properties make the brain susceptible to PCB-induced injury, as PCBs are recognized as potent inducers of oxidative stress (Choi et al., 2003; Choi et al., 2010). In fact, a recent study published by our group indicated that PCB153 can induce cellular oxidation acting through the NADPH oxidase complex (Eum et al., 2009). Moreover, exposure to particulate matter can also induce production of reactive oxygen species (ROS) in rat brain capillaries, resulting in alterations of expression of TJ proteins (Hartz et al., 2008). An increase in oxidative stress may provide a common trigger for downstream events that regulate BBB integrity. For example, oxidative stress-induced alterations of TJ proteins may act through Ras and Rho redox responsive elements (Haorah et al., 2007). Upon

activation, Rho phosphorylates downstream molecules such as Rho kinase (ROCK), which then results in increased myosin light chain (MLC) phosphorylation via inhibition of MLC phosphatases (Pellegrin and Mellor, 2007). Oxidative stress can also lead to the elevation of chemokine receptors at the brain endothelium, further contributing to MLC phosphorylation through the activation of myosin light chain kinase (MLCK) (Shiu et al., 2007). MLCK can modulate actin structure and phosphorylate TJ proteins, which results in the cytoskeletal reorganization. Under conditions of oxidative stress, activated protein tyrosine kinases (PTKs) may also trigger activation of matrix metalloproteinases (MMPs), which can degrade the endothelium basement membrane, leading to the disruption of the BBB (Rosenberg et al., 1998).

Recent reports from our laboratory implicate the brain endothelium as an important target of vascular toxicity of PCBs. Indeed, exposure to specific PCB congeners, including PCB153, stimulate induction of adhesion molecules and induce leukocyte adhesion (Eum et al., 2009; Sipos et al., 2012). These effects are important because inflammatory responses involving cerebral vessels contribute to the development of neuroinflammation, constitute the risk of onset of stroke, and potentiate tissue damage in brain ischemia/reperfusion (Lo et al., 2003). Upregulation of ICAM-1 and VCAM-1 expression by brain endothelial cells has also been associated with multiple sclerosis, encephalitis, and other inflammatory conditions in the brain (de Vries et al., 1997). Therefore, it is of significant clinical relevance that exposure to PCB153-NPs results in more pronounced expression of proinflammatory mediators as compared to treatment with PCB153 alone. Overexpression of inflammatory cytokines, such as TNF-α and IL-1β, can further stimulate production of proinflammatory mediators, impair BBB functions, and recruit inflammatory cells. Moreover, inflammatory cytokines can induce expression of adhesion molecules on endothelial cells, facilitating the adherence of leukocytes to the brain endothelium. A functional BBB is critical in maintaining the immune-privileged status of the brain. Thus, a strategy targeting inhibition of proinflammatory mediators may help to protect against PCB- or other environment pollutant-induced BBB dysfunction.

Increased expression of adhesion molecules results in enhanced adhesive properties of endothelial cells and stimulation of adhesion of leukocytes to the brain endothelium (Albelda et al., 1994; Wong et al., 2007). Therefore, we investigated the influence of PCB153 and/or NPs on leukocyte adhesion using both *in vivo* and *in vitro* models. Visualization of leukocyte-endothelium interaction was accomplished *in vivo* by detection of labeled leukocytes by fluorescent microscopy via a cranial window. While this method is suitable to study the interactions of leukocytes with brain microvessels, *in vitro* modeling of transendothelial migration of monocyte allows for quantitative comparison among different treatments.

Consistent with the effects on expression of pro-inflammatory mediators, both acute and chronic administration of PCB153-NPs significantly upregulate monocyte attachment to the brain endothelium, with PCB153 having only a moderate effect. These results indicate that brain microvessels can recognize and respond to PCB153-NPs by producing pro-inflammatory molecules. This response may serve as a pro-inflammatory sensor and ultimately distribute ROS and cytokines, further contributing to the CNS pathology.

Enhanced cerebrovascular toxicity of PCB153-NPs, as compared to PCB153 alone, may result from more effective bioaccumulation of these toxicants. The properties of NPs as effective carriers across the BBB are well described and have been used for drug delivery into the brain (Lockman et al., 2002). Another possibility is lower excretion rate of PCB153-NPs due to the longer retention of NPs (El-Ansary and Al-Daihan, 2009). Indeed, we observed a higher PCB153 body burden in animals chronically exposed to PCB153-NPs

than in PCB153 alone. These measurements were performed in adipose tissue to reflect lifetime PCB bioaccumulation (Crinnion, 2011). Because chronic exposure to PCB153 and/or NPs was administered, effects of PCB153 and NPs on intestinal epithelium might also contribute to increased PCB153 absorption into the blood stream. In fact, we recently demonstrated that oral exposure to PCBs can disrupt TJ proteins in small intestine and increase intestinal permeability (Choi et al., 2010).

Epidemiologic studies and laboratory evidence demonstrate that exposure to PCBs may enhance the risk for stroke and other vascular disorders (Hennig et al., 2005; Shcherbatykh et al., 2005). Therefore, one aim of the present study was to investigate the effects of PCB153 and/or NPs on the development and outcome of stroke. We detected a larger stroke volume in mice exposed to PCB153-NPs, as compared to other treatment groups, which was consistent with the effects of these toxicants on TJ protein expression and proinflammatory responses. Indeed, endothelial activation, proinflammatory and prothrombotic interactions between the vessel wall and circulating blood constituents are known risk factors triggering the onset of stroke (Stanimirovic and Satoh, 2000).

In summary, we demonstrate for the first time that binding of PCB153 to silica NPs can increase cerebrovascular toxicity of these toxicants by enhancing proinflammatory responses and disruption of the BBB integrity. These effects appear to predispose mice to stroke and potentiate brain injury associated with ischemia/reperfusion. Our results also emphasize the importance of risk assessment for NPs by demonstrating that even chemically inert silica NPs can markedly influence toxicity of other environmental chemicals, such as PCBs.

Acknowledgments

This study was supported by the grants from the National Institutes of Health (NIH) ES07380, CA133257, MH63022, MH072567, and DA027569. We would like to thank Dr. Yinan Wei (Department of Chemistry, University of Kentucky) for PCB analysis.

References

Abbott NJ, Ronnback L, Hansson E. Astrocyte-endothelial interactions at the blood-brain barrier. Nat Rev Neurosci. 2006; 7:41–53. [PubMed: 16371949]

Albelda SM, Smith CW, Ward PA. Adhesion molecules and inflammatory injury. FASEB J. 1994; 8:504–512. [PubMed: 8181668]

Alexander JS, Elrod JW. Extracellular matrix, junctional integrity and matrix metalloproteinase interactions in endothelial permeability regulation. J Anat. 2002; 200:561–574. [PubMed: 12162724]

ATSDR (Agency for Toxic Substances and Disease Registry). Health Consultation: Evaluation of Soil, Blood, and Air Data from Anniston, Alabama, Calhoun County, Alabama. Atlanta, GA: ATSDR; 2000. http://www.atsdr.cdc.gov/hac/pha/pha.asp?docid=930&pg=0

Borm PJ, Robbins D, Haubold S, Kuhlbusch T, Fissan H, Donaldson K, Schins R, Stone V, Kreyling W, Lademann J, Krutmann J, Warheit D, Oberdorster E. The potential risks of nanomaterials: a review carried out for ECETOC. Part Fibre Toxicol. 2006; 3:11. [PubMed: 16907977]

Calderon-Garciduenas L, Solt AC, Henriquez-Roldan C, Torres-Jardon R, Nuse B, Herritt L, Villarreal-Calderon R, Osnaya N, Stone I, Garcia R, Brooks DM, Gonzalez-Maciel A, Reynoso-Robles R, Delgado-Chavez R, Reed W. Long-term air pollution exposure is associated with neuroinflammation, an altered innate immune response, disruption of the blood-brain barrier, ultrafine particulate deposition, and accumulation of amyloid beta-42 and alpha-synuclein in children and young adults. Toxicol Pathol. 2008; 36:289–310. [PubMed: 18349428]

Campelo JM, Luna D, Luque R, Marinas JM, Romero AA. Sustainable preparation of supported metal nanoparticles and their applications in catalysis. ChemSusChem. 2009; 2:18–45. [PubMed: 19142903]

Chen L, Swartz KR, Toborek M. Vessel microport technique for applications in cerebrovascular research. J Neurosci Res. 2009; 87:1718–1727. [PubMed: 19115415]

Chen L, Zhang B, Toborek M. Autophagy is involved in nanoalumina-induced cerebrovascular toxicity. Nanomedicine. 2012

Chen L, Choi JJ, Choi YJ, Hennig B, Toborek M. HIV-1 Tat-induced cerebrovascular toxicity is enhanced in mice with amyloid deposits. Neurobiol Aging. 2011

Choi W, Eum SY, Lee YW, Hennig B, Robertson LW, Toborek M. PCB 104-induced proinflammatory reactions in human vascular endothelial cells: relationship to cancer metastasis and atherogenesis. Toxicol Sci. 2003; 75:47–56. [PubMed: 12805654]

Choi YJ, Seelbach MJ, Pu H, Eum SY, Chen L, Zhang B, Hennig B, Toborek M. Polychlorinated biphenyls disrupt intestinal integrity via NADPH oxidase-induced alterations of tight junction protein expression. Environ Health Perspect. 2010; 118:976–981. [PubMed: 20299304]

Chrysikou LP, Gemenetzis PG, Samara CA. Wintertime size distribution of polycyclic aromatic hydrocarbons (PAHs), polychlorinated biphenyls (PCBs) and organochlorine pesticides (OCPs) in the urban environment: Street- vs rooftop-level measurements. Atmospheric Environment. 2009; 43:290–300.

Crinnion WJ. Polychlorinated Biphenyls: Persistent Pollutants with Immunological, Neurological, and Endocrinological Consequences. Alternative Medicine Review. 2011; 16:5–13. [PubMed: 21438643]

de Vries HE, Kuiper J, de Boer AG, Van Berkel TJ, Breimer DD. The blood-brain barrier in neuroinflammatory diseases. Pharmacol Rev. 1997; 49:143–155. [PubMed: 9228664]

Dziennis S, Yang D, Cheng J, Anderson KA, Alkayed NJ, Hurn PD, Lein PJ. Developmental exposure to polychlorinated biphenyls influences stroke outcome in adult rats. Environ Health Perspect. 2008; 116:474–480. [PubMed: 18414629]

El-Ansary A, Al-Daihan S. On the toxicity of therapeutically used nanoparticles: an overview. J Toxicol. 2009; 2009:754810. [PubMed: 20130771]

Eum SY, Andras I, Hennig B, Toborek M. NADPH oxidase and lipid raft-associated redox signaling are required for PCB153-induced upregulation of cell adhesion molecules in human brain endothelial cells. Toxicol Appl Pharmacol. 2009; 240:299–305. [PubMed: 19632255]

Fu S, Cheng HX, Liu YH, Yang ZZ, Xu XB. Spatial character of polychlorinated biphenyls from soil and respirable particulate matter in Taiyuan, China. Chemosphere. 2009; 74:1477–1484. [PubMed: 19111889]

Fullerton SM, Shirman GA, Strittmatter WJ, Matthew WD. Impairment of the blood-nerve and blood-brain barriers in apolipoprotein e knockout mice. Exp Neurol. 2001; 169:13–22. [PubMed: 11312553]

Goncharov A, Bloom M, Pavuk M, Birman I, Carpenter DO. Blood pressure and hypertension in relation to levels of serum polychlorinated biphenyls in residents of Anniston, Alabama. J Hypertens. 2010; 28:2053–2060. [PubMed: 20644494]

Hansen LG. Stepping backward to improve assessment of PCB congener toxicities. Environ Health Perspect. 1998; 106(Suppl 1):171–189. [PubMed: 9539012]

Haorah J, Ramirez SH, Schall K, Smith D, Pandya R, Persidsky Y. Oxidative stress activates protein tyrosine kinase and matrix metalloproteinases leading to blood-brain barrier dysfunction. J Neurochem. 2007; 101:566–576. [PubMed: 17250680]

Hartz AM, Bauer B, Block ML, Hong JS, Miller DS. Diesel exhaust particles induce oxidative stress, proinflammatory signaling, and P-glycoprotein up-regulation at the blood-brain barrier. FASEB J. 2008; 22:2723–2733. [PubMed: 18474546]

Hawkins BT, Davis TP. The blood-brain barrier/neurovascular unit in health and disease. Pharmacol Rev. 2005; 57:173–185. [PubMed: 15914466]

Hawkins BT, Egleton RD. Pathophysiology of the blood-brain barrier: animal models and methods. Curr Top Dev Biol. 2008; 80:277–309. [PubMed: 17950377]

Hennig B, Reiterer G, Majkova Z, Oesterling E, Meerarani P, Toborek M. Modification of environmental toxicity by nutrients: implications in atherosclerosis. Cardiovasc Toxicol. 2005; 5:153–160. [PubMed: 16046791]

Lake JL, Mckinney R, Lake CA, Osterman FA, Heltshe J. Comparisons of Patterns of Polychlorinated Biphenyl Congeners in Water, Sediment, and Indigenous Organisms from New-Bedford Harbor, Massachusetts. Archives of Environmental Contamination and Toxicology. 1995; 29:207–220.

Lee YW, Eum SY, Chen KC, Hennig B, Toborek M. Gene expression profile in interleukin-4-stimulated human vascular endothelial cells. Mol Med. 2004; 10:19–27. [PubMed: 15502879]

Lo EH, Dalkara T, Moskowitz MA. Mechanisms, challenges and opportunities in stroke. Nat Rev Neurosci. 2003; 4:399–415. [PubMed: 12728267]

Lockman PR, Mumper RJ, Khan MA, Allen DD. Nanoparticle technology for drug delivery across the blood-brain barrier. Drug Dev Ind Pharm. 2002; 28:1–13. [PubMed: 11858519]

Lockman PR, Koziara JM, Mumper RJ, Allen DD. Nanoparticle surface charges alter blood-brain barrier integrity and permeability. Journal of Drug Targeting. 2004; 12:635–641. [PubMed: 15621689]

Napierska D, Thomassen LC, Rabolli V, Lison D, Gonzalez L, Kirsch-Volders M, Martens JA, Hoet PH. Size-dependent cytotoxicity of monodisperse silica nanoparticles in human endothelial cells. Small. 2009; 5:846–853. [PubMed: 19288475]

Nemmar A, Inuwa IM. Diesel exhaust particles in blood trigger systemic and pulmonary morphological alterations. Toxicol Lett. 2008; 176:20–30. [PubMed: 17980520]

Nisbet IC, Sarofim AF. Rates and Routes of Transport of PCBs in the Environment. Environ Health Perspect. 1972; 1:21–38. [PubMed: 17539082]

Norstrom K, Czub G, McLachlan MS, Hu D, Thorne PS, Hornbuckle KC. External exposure and bioaccumulation of PCBs in humans living in a contaminated urban environment. Environ Int. 2010; 36:855–861. [PubMed: 19394084]

Oberdorster G, Sharp Z, Atudorei V, Elder A, Gelein R, Kreyling W, Cox C. Translocation of inhaled ultrafine particles to the brain. Inhal Toxicol. 2004; 16:437–445. [PubMed: 15204759]

Pellegrin S, Mellor H. Actin stress fibres. J Cell Sci. 2007; 120:3491–3499. [PubMed: 17928305]

Peters A, Veronesi B, Calderon-Garciduenas L, Gehr P, Chen LC, Geiser M, Reed W, Rothen-Rutishauser B, Schurch S, Schulz H. Translocation and potential neurological effects of fine and ultrafine particles a critical update. Part Fibre Toxicol. 2006; 3:13. [PubMed: 16961926]

Prince MM, Ruder AM, Hein MJ, Waters MA, Whelan EA, Nilsen N, Ward EM, Schnorr TM, Laber PA, Davis-King KE. Mortality and exposure response among 14,458 electrical capacitor manufacturing workers exposed to polychlorinated biphenyls (PCBs). Environ Health Perspect. 2006; 114:1508–1514. [PubMed: 17035134]

Roberts JW, Dickey P. Exposure of children to pollutants in house dust and indoor air. Rev Environ Contam Toxicol. 1995; 143:59–78. [PubMed: 7501867]

Rosenberg GA, Estrada EY, Dencoff JE. Matrix metalloproteinases and TIMPs are associated with blood-brain barrier opening after reperfusion in rat brain. Stroke. 1998; 29:2189–2195. [PubMed: 9756602]

Saghir SA, Hansen LG, Holmes KR, Kodavanti PR. Differential and non-uniform tissue and brain distribution of two distinct 14C-hexachlorobiphenyls in weanling rats. Toxicol Sci. 2000; 54:60–70. [PubMed: 10746932]

Seelbach M, Chen L, Powell A, Choi YJ, Zhang B, Hennig B, Toborek M. Polychlorinated biphenyls disrupt blood-brain barrier integrity and promote brain metastasis formation. Environ Health Perspect. 2010; 118:479–484. [PubMed: 20064788]

Shcherbatykh I, Huang X, Lessner L, Carpenter DO. Hazardous waste sites and stroke in New York State. Environ Health. 2005; 4:18. [PubMed: 16129026]

Shiu C, Barbier E, Di Cello F, Choi HJ, Stins M. HIV-1 gp120 as well as alcohol affect blood-brain barrier permeability and stress fiber formation: involvement of reactive oxygen species. Alcohol Clin Exp Res. 2007; 31:130–137. [PubMed: 17207111]

Silverstone AE, Rosenbaum PF, Weinstock RS, Bartell SM, Foushee HR, Shelton C, Pavuk M. Polychlorinated biphenyl (PCB) exposure and diabetes: results from the Anniston Community Health Survey. Environ Health Perspect. 2012; 120:727–732. [PubMed: 22334129]

Sipka S, Eum SY, Son KW, Xu S, Gavalas VG, Hennig B, Toborek M. Oral administration of PCBs induces proinflammatory and prometastatic responses. Environ Toxicol Pharmacol. 2008; 25:251–259. [PubMed: 18438459]

Sipos E, Chen L, Andras IE, Wrobel J, Zhang B, Pu H, Park M, Eum SY, Toborek M. Proinflammatory adhesion molecules facilitate polychlorinated biphenyl-mediated enhancement of brain metastasis formation. Toxicol Sci. 2012; 126:362–371. [PubMed: 22240979]

Stanimirovic D, Satoh K. Inflammatory mediators of cerebral endothelium: a role in ischemic brain inflammation. Brain Pathol. 2000; 10:113–126. [PubMed: 10668901]

Valavanidis A, Fiotakis K, Vlachogianni T. Airborne particulate matter and human health: toxicological assessment and importance of size and composition of particles for oxidative damage and carcinogenic mechanisms. J Environ Sci Health C Environ Carcinog Ecotoxicol Rev. 2008; 26:339–362. [PubMed: 19034792]

Wong D, Prameya R, Dorovini-Zis K. Adhesion and migration of polymorphonuclear leukocytes across human brain microvessel endothelial cells are differentially regulated by endothelial cell adhesion molecules and modulate monolayer permeability. J Neuroimmunol. 2007; 184:136–148. [PubMed: 17291598]

Yamada H, Takayanagi K, Tateishi M, Tagata H, Ikeda K. Organotin compounds and polychlorinated biphenyls of livers in squid collected from coastal waters and open oceans. Environ Pollut. 1997; 96:217–226. [PubMed: 15093421]

Zhang B, Chen L, Swartz KR, Bruemmer D, Eum SY, Huang W, Seelbach M, Choi YJ, Hennig B, Toborek M. Deficiency of telomerase activity aggravates the blood-brain barrier disruption and neuroinflammatory responses in a model of experimental stroke. J Neurosci Res. 2010; 88:2859–2868. [PubMed: 20564349]

Zhong Y, Smart EJ, Weksler B, Couraud PO, Hennig B, Toborek M. Caveolin-1 regulates human immunodeficiency virus-1 Tat-induced alterations of tight junction protein expression via modulation of the Ras signaling. J Neurosci. 2008; 28:7788–7796. [PubMed: 18667611]

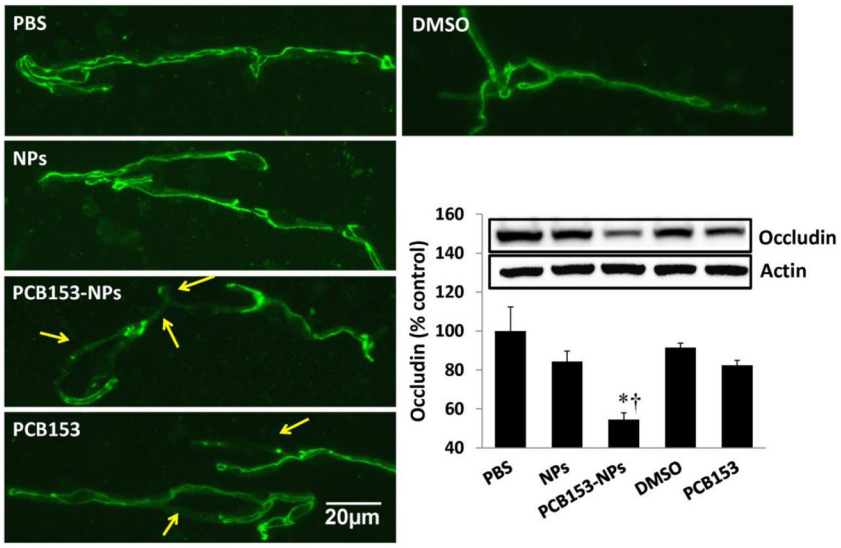

Figure 1A

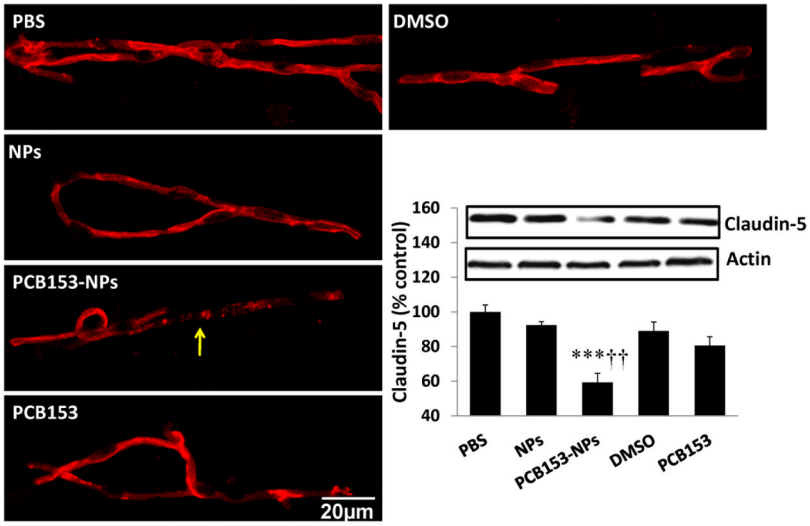

Figure 1B

Figure 1. Treatment with PCB153-NPs disrupts expression of tight junction proteins and BBB integrity

Mice were exposed to PCB153-NPs by infusion into the internal carotid artery (ICA) at the dose of 5 ng PCB153/g body weight bound to 1.04×10^5 silica NPs. Control mice were infused with the same amounts of NPs, PCB153 dissolved in DMSO, or vehicle (PBS or 0.01% DMSO). Brain microvessels were isolated 24 h post treatment and analyzed for occludin (A) and claudin-5 (B) expression by immunoblotting and immunofluorescence. Immunoreactivity of occludin and claudin-5 was stained in green and red, respectively; scale bar=20 μm. The blots in A and B are representative images from all experiments and the quantified results are depicted in the form of bar graphs. Arrows indicate disrupted continuity of tight junction proteins. Results are mean ± SEM, n=4. *Significantly different

as compared to control groups at *p<0.05 or ***p<0.001. †Results in the PCB153-NP group are statistically different from those in the PCB153 group at †p<0.05 or †††p<0.001.

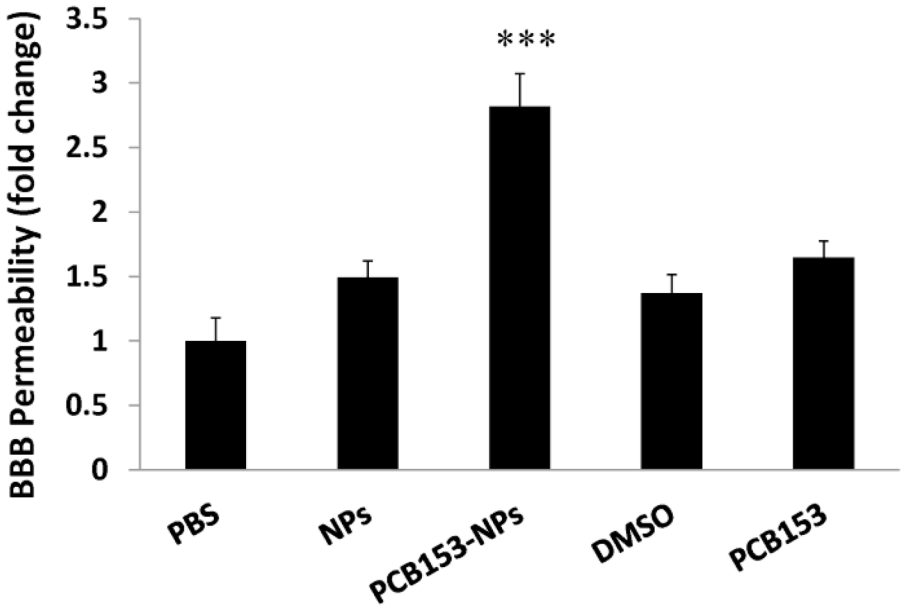

Figure 2. Treatment with PCB153-NPs increases permeability of the BBB

Mice were injected with vehicle, PCB153 and/or NPs as in Figure 1. BBB permeability was evaluated using sodium fluorescein 24 h post treatment. Results are mean ±SEM, n=4. ***Significantly different as compared to other groups at $p<0.001$.

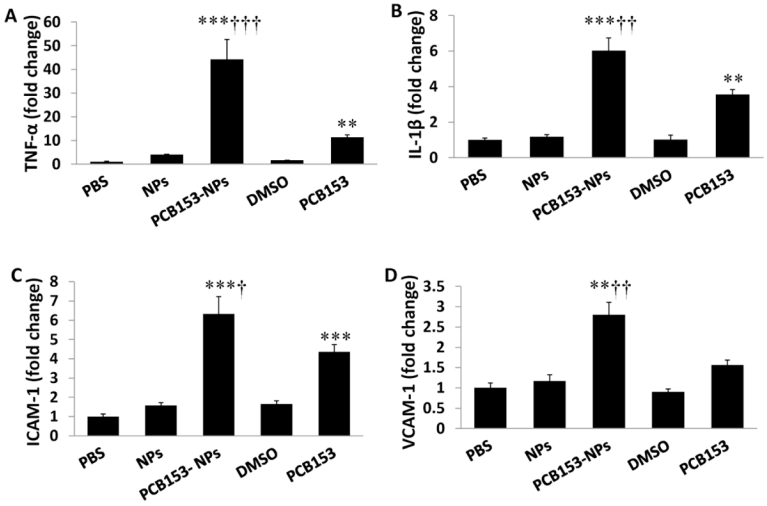

Figure 3. Exposure to PCB153-NPs potentiates inflammatory responses in brain capillaries

Mice were treated as in Figure 1, followed by brain microvessel isolation. mRNA levels of TNF-α (A), IL-1β (B), ICAM-1 (C), and VCAM-1 (D) were determined by real-time PCR. Results are mean ± SEM, n=6. *Significantly different as compared to control groups at **$p<0.01$ or ***$p<0.001$. †Results in the PCB153-NPs group are statistically different from those in the PCB153 group at $^{\dagger}p<0.05$, $^{\dagger\dagger}p<0.01$, or $^{\dagger\dagger\dagger}p<0.001$.

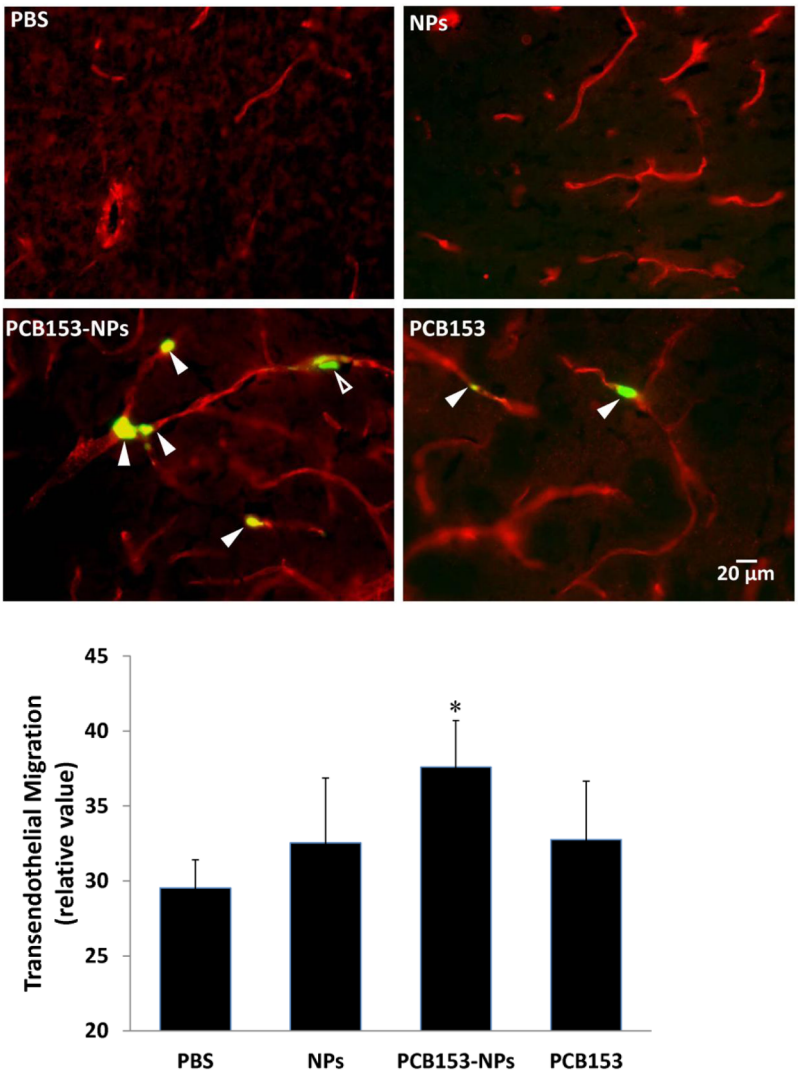

Figure 4. Treatment with PCB153-NPs enhances monocyte transmigration

(A) Mice were exposed to vehicle, PCB153, and/or NPs as in Figure 1, followed by injection with monocytic J774.1 cells labeled with CFDA-SE (green) into the internal carotid artery. In addition, brain sections were stained for claudin-5 (red) to visualize the vessels. Closed arrowheads indicate labeled J774.1 cells inside cerebral vessels, while open arrowheads indicate labeled J774.1 cells that appear to be present in the perivascular space. Scale bar = 20 μm. (B) Con uent hCMEC/D3 cells cultured on Transwell inserts were treated with PCB153-NPs (PCB153, 1.6 μM; NPs, 2.08×10^5), PCB153 (1.6 μM), NPs (2.08×10^5), or vehicle for 24 h. THP-1 monocytic cells were labeled with calcein AM, added on the top of endothelial monolayers, and their transendothelial migration was assessed 4 h later. Data are mean ± standard deviation (SD), n=6. *Significantly different as compared to control groups at $p<0.05$.

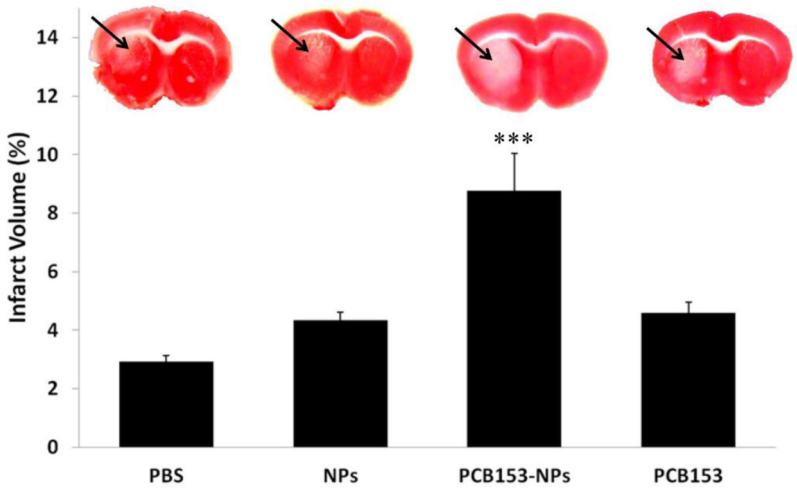

Figure 5. Exposure to PCB153-NPs increases the infarct volume in the experimental stroke model

Mice were treated as in Figure 1 and subjected to a 40 min MCAO, followed by a 24 h reperfusion, and staining with 2,3,5-triphenyltetrazolium chloride (TTC) to visualize viable tissue. Unstained area (arrows) corresponds to damaged brain tissue. Quantified results of negative TTC staining are depicted in the form of bar graphs. Results are mean ± SEM, n=5–7. ***Significantly different as compared to other groups at $p<0.001$.

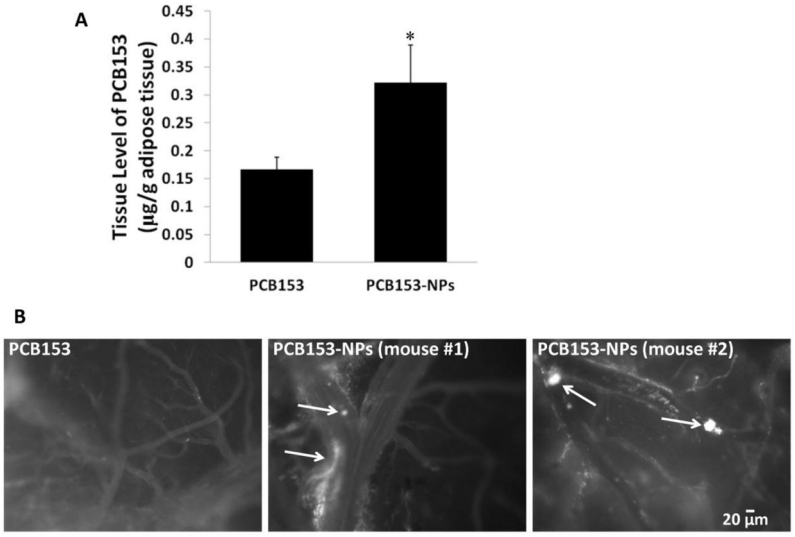

Figure 6. Long-term exposure to PCB153-NPs potentiates PCB153 adipose accumulation and leukocyte attachment to cerebral vessels

(A) Mice were exposed orally to PCB153-NPs (5 ng PCB153/g body weight bound to 1.04 × 10^5 silica NPs), the equimolar dose of PCB153, or the appropriate vehicles for 30 days. PCB153 levels were assessed in adipose tissue. Results are mean ± SEM, n=5–6. *Significantly different as compared to other groups at $p<0.05$. (B) Mice were exposed as in (A), followed by installation of the cranial window. Circulating leukocytes were fluorescently labeled by i.p. injection with rhodamine 6G and the interactions of labeled leukocytes with the brain endothelium were detected via cranial window under fluorescent microscope. Arrows indicate leukocytes inside the cerebral vessels that appear to be attached to the brain endothelium. Scale bar = 20 μm.

Table 1

Hydrodynamic particle diameters of NPs in different media as determined by dynamic light scattering.

Particles	Z-Average Diameter (nm)	PDI
NPs		
Water	346.5	0.246
PBS	346.3	0.610
EBM-2	333.6	0.294
PCB153-NPs		
Water	246.7	0.277
PBS	265.8	0.442
EBM-2	239.5	0.511